Trop J Nat Prod Res, January 2026; 10(1): 6876 - 6888

ISSN 2616-0684 (Print)
ISSN 2616-0692 (Electronic)

Tropical Journal of Natural Product Research

Available online at https://www.tjnpr.org

Original Research Article

Evaluation of Antimicrobial Potential of Endophytic Fungi and LC-MS/MS Profiling of Metabolites from *Senna alata* (L.) Roxb.

Muh Anugrawan[1]*, Yanti Leman[2], Isra Wahid[3], Yulia Yusrini Djabir[4], Anna Khuzaimah[5]

[1]*Biomedical Science Study Program, Postgraduate School, Hasanuddin University, Tamalanrea, Makassar 90245, Indonesia.*
[2]*Department of Pharmacology, Faculty of Medicine, Hasanuddin University, Tamalanrea, Makassar 90245, Indonesia*
[3]*Department of Parasitology, Faculty of Medicine, Hasanuddin University, Tamalanrea, Makassar 90245, Indonesia.*
[4]*Department of Pharmacy, Faculty of Pharmacy, Hasanuddin University, Tamalanrea, Makassar 90245, Indonesia.*
[5]*Departement of Nutrition Science, Faculty of Public Health, Hasanuddin University, Tamalanrea, Makassar 90245, Indonesia.*

ARTICLE INFO

Article history:
Received 30 October 2025
Revised 15 January 2026
Accepted 22 January 2026
Published online 01 February 2026

Copyright: © 2026 Anugrawan *et al*. This is an open-access article distributed under the terms of the Creative Commons Attribution License, which permits unrestricted use, distribution, and reproduction in any medium, provided the original author and source are credited.

ABSTRACT

The rise of antimicrobial resistance necessitates the discovery of novel bioactive sources. This study evaluated the antimicrobial potential of endophytic fungi isolated from *Senna alata* (L.) Roxb. leaves and profiled their secondary metabolites using LC-MS/MS. Endophytic fungi were isolated and subjected to antagonistic assays. The promising endophytic fungi were then identified morphologically and molecularly. Antibacterial activity was evaluated against bacterial and pathogenic fungal strains, while LC-MS/MS characterized the metabolite profiles of the endophytic fungi. Seven fungal isolates from *S. alata* leaves (SA-1 to SA-7) were obtained and screened for antagonistic activity via agar-plug (disk-diffusion agar assays) and fermentation broth (well-diffusion agar assays). Endophytic fungal SA-5 exhibited the most sustained and broad-spectrum inhibition, with zones of 13.93–18.12 mm against bacteria and 15.19 mm against *Malassezia furfur* in the ethyl acetate extract, while its aqueous extract inhibited *Candida albicans* at ≥ 10 mg/mL (12.93–15.33 mm). Molecular identification based on ITS sequencing confirmed SA-5 as *Phomopsis* sp. (99.46 % identity). Bioactive crude extracts from SA-5 reveal 29 metabolites, including naringenin, Asiatic acid, coumarin, indole-3-carboxaldehyde, and feruloyl putrescine. These findings position *Phomopsis* sp., SA-5 as a promising source of structurally diverse antimicrobial agents. Future work should focus on elucidating its biosynthetic pathways and *in vivo* pharmacological mechanisms to advance the development of plant-derived antifungal and antibacterial therapeutics.

Keywords: antimicrobial, endophytic fungi, *Phomopsis* sp., secondary metabolite, *Senna alata* (L.) Roxb

Introduction

Endophytic fungi are a group of fungi that live partially or entirely within the tissues of living plants. These fungi often do not pose a threat to their host and instead produce beneficial secondary metabolites with antimicrobial, immunosuppressive, antidiabetic, anticancer, insecticidal, and antiviral properties.[1-3] Due to genetic transfer between endophytic fungi and their host plants, endophytic fungi can produce bioactive compounds and secondary metabolites that are identical to, different from, or even superior to those of their host plants. As a result, endophytic fungi tend to generate valuable and unique substances.[4,5] Moreover, endophytic fungi also have a short life cycle and can produce large amounts of bioactive compounds, making them a natural, economical, and environmentally friendly source of medicinal substances.[2,6], This methed of harnessing the great potential of relationships between endophytic fungi and their host plants offers a means of finding new antimicrobial drugs and answering the urgent need for effective treatment.[7] The search for novel bioactive natural products has increasingly highlighted endophytic microorganisms as highly promising sources, owing to their remarkable genetic diversity and yet largely unexplored metabolic potential.

*Corresponding author. Email: anugrawanahmar@gmail.com
Tel: +62 823-3656-3148

Citation: Anugrawan M, Leman Y, Wahid I, Djabir YY, Khuzaimah A. Evaluation of antimicrobial potential of endophytic fungi and LC-MS/MS profiling of metabolites from *Senna alata* (L.) Roxb. Trop J Nat Prod Res. 2026; 10(1): 6876 – 6888 https://doi.org/10.26538/tjnpr/v10i1.59

Official Journal of Natural Product Research Group, Faculty of Pharmacy, University of Benin, Benin City, Nigeria

Endophytes have emerged as valuable biological systems for understanding host–microbe interactions and as effective mediators in the discovery of structurally unique and pharmacologically significant secondary metabolites. Consequently, they represent a productive and reliable reservoir for the development of new therapeutic leads in medicine, pharmaceuticals, and biotechnology, particularly in addressing emerging and recurrent health challenges. Endophytic fungi, in particular, are known to produce a wide spectrum of bioactive compounds, including steroids, alkaloids, terpenoids, quaternary metabolites, isocoumarins, quinone derivatives, phenolic compounds, flavans, xanthones, and various peptides, many of which exhibit antimicrobial, antimalarial, antiviral, and anticancer activities. This expanding biochemical diversity underscores the importance of continued exploration of endophytic fungi as strategic platforms for natural product discovery and drug development.[8]

Candle bush, or ringworm bush, *Senna alata* L., has medicinal potential for treating fungal and bacterial infections. Its leaves are commonly used as medicine by rubbing them on the skin or crushing them and applying them to infected areas. The main active compounds identified in leaves of *S. alata*, include alkaloids, saponins, tannins, anthraquinones, and flavonoids.[9] These chemical constituents contributes to its bioactivity, i.e. anti-inflammatory, anti-allergic, antimicrobial, and antioxidant properties, and they are effective against several types of fungi. .[10]reported that the ethanol extract of leaves of *S. alata* has shown antimicrobial efficacy against seven clinical bacterial strains, including *Bacillus cereus, B. subtilis, Staphylococcus aureus, S. epidermidis, Escherichia coli, Klebsiella pneumoniae* and *Proteus vulgaris.*[10]

According to .[11] the leaf ethanol extract of *S. alata* at 20% exhibited antibacterial activity against *S. aureus, S. epidermidis, P. aeruginosa*, and *P. acnes*, with the inhibition zone diameters of 20.03, 30.28, 17.49,

© 2026 the authors. This work is licensed under the Creative Commons Attribution 4.0 International License

and 17.03 mm, respectively.[11] Research by [12] demonstrated that the effectiveness of *S. alata* leaves at a 50% concentration is comparable to 2% ketoconazole, suggesting its potential as a plant-based alternative to synthetic antimicrobials.[12] [13] indicated that *S. alata* leaves contain bioactive chemicals associated with significant antibacterial efficacy against Methicillin-resistant *Staphylococcus aureus* (MRSA).[13] Beyond its phytochemical constituents, the endophytic fungi residing within *S. alata* leaves may be recognized for their ability to produce unique metabolite compounds. These metabolites can be predicted and characterized through molecular modeling approaches, offering insights into their mechanisms of action and potential as antimicrobial agents.

This study aims to profile and analyze the metabolite compounds produced by endophytic fungi isolated from the leaves of *S. alata*, with a specific focus on their potential antimicrobial activity. Through molecular modeling and bioactivity screening, the research seeks to identify bioactive metabolites that may be candidates for developing novel, plant-based antimicrobial agents. This study represents the inaugural integration of antagonistic screening, molecular identification, and LC-MS/MS metabolite profiling of endophytic fungus derived from *S. alata* leaves.

Materials and Methods

Materials

Potato Dextrose Agar (PDA), Potato Dextrose Broth (PDB), Mueller Hinton Agar (MHA), Nutrient Agar (NA), Nutrient Broth (NB), Sabouraud Dextrose Agar (SDA) and Yeast ekstract were brought from Himedia. Nukleon PHYTOPure kit was purchased from Amersham LIFE SCIENCE. Primer Forward ITS 1 and Reverse ITS 4 were brought from Macrogen. GoTaq Green Master Mix 2X and TAE buffer from Promega. Quick-DNA MagBead Plus Kit from Zymo Research.

Bacterial and Fungal Test Organisms

The bacterial strains *P. aeruginosa* (ATCC 27853) and *S. aureus* (ATCC 2913) were used as test cultures in NA and MHA. The bacterial cultures were first placed on NA and incubated at 37 ℃ for 24 h. Furthermore, the fungus strains *Candida albican* (ATCC 14053) and *Malassezia furfur (*ATCC 14521) were used as a test culture in PDA and SDA and incubated at 25 ℃ for 72 h.

Sample collection and identification

The leaves were collected from Maritengngae District (3°58’25.5” S 119°47’18.5” E), Sidenreng Rappang Regency, South Sulawesi, Indonesia on January 18, 2025. The plant was identified at the Laboratory of Traditional Medicine Raw Materials, National Research and Innovation Agency (BRIN) in Cibinong, West Java, Indonesia (ID code 201543 and sample No. 6449-201543-1). The endophytic fungi were isolated using mature leaf tissue. Leaves were selectively harvested in pristine condition-intact, free from physical damage, unaffected by insect predation, and devoid of pesticides or external contaminants such as soil, sand, or dust.

Isolation of endophytic fungi

A sterilization procedure was used on the leaves' surface to avoid contamination. The fresh leaves were rinsed sequentially with running tap water, Tween 20, 70% ethanol, and sodium hypochlorite (1:3). Subsequently, the samples were rewashed with 70% ethanol and sterile distilled water, then air-dried.[14] The leaves were cut into 1 cm using a sterile scalpel in a laminar air flow (Scitek, China). The segments were then inoculated on sterile PDA supplemented with 0.05% chloramphenicol and incubated at room temperature (25 ℃) for 7 days. Fungal growth surrounding the leaf tissue was observed as an indication of endophytic fungal development. The fungal growth surrounding the plant leaves was sub-cultured onto PDA supplemented with 0.05% chloramphenicol. Colony morphology and pigmentation were observed until pure isolates were obtained. Each colony exhibiting a distinct shape or color was subsequently transferred to fresh PDA.[15] A total of seven isolates endophytic fungal were successfully obtained from *S. alata* leaves, coded SA-1 to SA-7.

Morphological identification of the endophytic fungus

Macroscopic identification of fungal isolates was conducted to examine colony morphology by direct visual observation, focusing on the shape and color of the colony surface and the edges of the Petri dish. The fungal isolates were collected using an inoculating needle and transferred onto sterile glass slides. A drop of lactophenol cotton blue solution was added, and the samples were examined microscopically under a light microscope (Olympus CX33 Series, Japan) at 100-400× magnification.[15]

Antagonist test

There were 2 methods employed in the screening of the endophytic fungi as a potential antimicrobial agent i.e. agar plug diffusion and the agar well diffusion method. The Agar plug diffusion method was carried out by placing the isolates upside-down in a petri dish containing the pathogenic bacteria and fungi, and the procedure is similar to that used in the disk-diffusion method.[16] The plates were incubated for 24 h at 37 ℃ and 72 h at 25 ℃. For the Agar well diffusion method, about 20 µL of the fermentation broth was collected on days 14, 18, and 21, then introduced into wells containing pathogenic bacteria. The plates were incubated for 24 h at 37 ℃ and 72 h at 25 ℃. However, only SA-5 showing significant effects were selected for further evaluation.

Molecular identification of SA-5 endophytic fungi

Extraction of DNA and amplification

Genomic DNA was isolated from approximately 35 µL of fungal mycelium—harvested in mid-log phase-using the Quick-DNA MagBead Plus Kit. Briefly, samples were suspended in 400 µL of lysis buffer and disrupted with 0.5 mm zirconia beads on a bead beater at 5,000 rpm for 2 × 40 s, then incubated with 20 µL Proteinase K at 56 ℃ for 30 min. After centrifugation, the supernatant was combined with 250 µL binding buffer (20% PEG-8000, 2.5 M NaCl) and 50 µL magnetic beads, incubated for 10 min at room temperature with gentle agitation, and washed twice with 500 µL of 80% ethanol. The DNA was eluted in 50 µL of prewarmed (37 ℃) elution buffer (10 mM Tris-HCl, pH 8.5). The yield and purity were assessed on a NanoDrop ND-2000 (A260/A280 = 1.8–2.0) and quantified via Qubit 3.0 Fluorometer (dsDNA HS assay). For PCR amplification of the internal transcribed spacer (ITS) region, 50 ng of genomic DNA was added to a 25 µL reaction containing 12.5 µL 2X Takara Ex Taq Master Mix (1.5 mM $MgCl_2$, 0.4 mM each dNTP), 0.5 µM ITS1 primer (5′-TCCGTAGGTGAACCTGCGG-3′), 0.5 µM ITS4 primer (3′-TCCTCCGCTTATTGATATGC-5′), and nuclease-free water. Amplification was performed on a Takara PCR System with an initial denaturation at 95 ℃ for 3 min, 38 cycles of 95 ℃ for 15 s, 52 ℃ for 30 s, 72 ℃ for 45 s, followed by a 3 min final extension at 72 ℃ and a 4 ℃ hold. PCR specificity and amplicon size (~600 bp) were confirmed on a 1.5% agarose gel in 1X TAE with GelRed, run at 100 V for 30 min. Before Sanger sequencing, products were purified with ExoSAP-IT to remove excess primers and dNTPs.

Electrophoresis

To separate and visualize PCR amplicons, a 2% (w/v) agarose gel was cast by dissolving 1 g of agarose in 100 mL of 1×TAE buffer in a heat-resistant flask, microwaving for 2 mins until fully liquefied, then cooling to approximately 60 ℃ before adding 8 µL of ethidium bromide (10 mg/mL). The molten gel was poured into a casting tray fitted with a comb and allowed to solidify at room temperature. Each PCR reaction (8 µL) was mixed with 2 µL of 6×loading dye, loaded into the wells, and submerged in 1×TAE buffer. Electrophoresis was run at 100 V for 50 min, and DNA bands were visualized under a UV transilluminator (SLB-01W, MaestroGen Inc., Hsinchu, Taiwan).

Sequencing and species identification using The Basic Local Alignment Search Tool (BLAST)

Sequencing of the PCR amplicons was outsourced to 1st Base at PT Genetika Indonesia. The single-pass DNA sequencing method was chosen to generate single-direction reads. Sequencing reactions employed the same ITS1 and ITS4 primers used in PCR amplification (Thermo Fisher Scientific, USA). Templates were prepared according to the provider standard Sanger sequencing protocol. Raw

© 2026 the authors. This work is licensed under the Creative Commons Attribution 4.0 International License

chromatogram files were delivered and imported into the BioEdit application for analysis. Chromatograms were visually inspected to assess signal quality and peak resolution. Low-quality terminal regions were trimmed based on ambiguous base calls. High-quality reads were aligned to produce final consensus sequences for each sample. Consensus sequences were queried against the NCBI nucleotide database using BLAST. Query coverage was evaluated to measure the percentage of the sequence aligned. Maximum percent identity scores were examined to identify the closest database matches—final organism identification integrated query coverage and maximum identity metrics.

Phylogenic Analysis
The sequence alignments were subsequently subjected to phylogenetic reconstruction using MEGA11 i.e. Molecular Evolutionary Genetics Analysis, Version 11 (MEGA software, USA-Japan) on Windows 11.

Cultivation and extraction of fungal metabolites
Pure fungal cultures were rejuvenated on slanted PDA and incubated at 25 °C for 3-12 days. Inoculum was collected from the slanted agar and transferred into eight Erlenmeyer flasks containing 100 mL of PDB supplemented with yeast extract. Fermentation was carried out under controlled conditions at 25 °C for 18 days.[1] Upon completion of fermentation, the cultures were filtered to separate the mycelial biomass from the culture broth. The culture broth was then subjected to liquid–liquid extraction with ethyl acetate (1:1, v/v) using a separatory funnel and shaken for 20 min to ensure efficient partitioning of extracellular metabolites. After phase separation, the ethyl acetate layer was collected and concentrated under reduced pressure using a rotary evaporator (Büchi, Germany) at 40 °C and approximately 170 mbar, yielding the ethyl acetate extract.[15] Following removal of the ethyl acetate phase, the remaining aqueous phase constituted the water extract, which was subsequently concentrated to dryness by lyophilization using a Lyovapor™ L-200 (Büchi, Germany).

Sample preparation
A stock solution was diluted with about 400 mg of ethyl acetate and water extracts in 2 mL of 5% DMSO (20%). About 500 µL of stock solution was transferred to another tube and added 500 µL of water (10%), and so on until 5 and 2.5% were achieved. In a paper disk (d=6), 20 µL of each sample was dropped and dried.

Antimicrobial activity of endophytic fungal crude extract
Fungal extracts from the SA-5 were subjected to agar disk diffusion to determine their antimicrobial activities against pathogenic bacteria and yeast. Bacterial cultures with an optical density of 0.5 at 600 nm were pipetted (100 µL) into pre-warmed MHA for the antibacterial assay. The mixture was homogenized and evenly distributed into sterile Petri dishes, then allowed to solidify at room temperature. Once solidified, sterile paper disks were placed on the surface of the agar. In the antifungal assay, fungal cultures standardized to 1 McFarland standard were pipetted (100 µL) into warm PDA, homogenized, and poured into Petri dishes. The agar was left to solidify before proceeding. Positive controls (gentamicin for bacteria and ketoconazole for fungi) and negative control (5% DMSO) were also applied to separate disks. All Petri dishes were incubated under appropriate conditions, and the diameter of the inhibition zones surrounding each disk was measured using a digital caliper with an accuracy of 0.01 mm.[17] Each test was conducted in independent triplicate. The antibacterial agent gentamicin (10 µg) and antifungal agent ketoconazole (30 µg) were included in the assays as positive standards.

LC-MS/MS analysis of secondary metabolites
Secondary metabolites in the most bioactive crude extract from the SA-5 endophytic fungal strain were characterized using LC–MS/MS (Q Exactive Plus Thermo Scientific, USA). Analysis was performed on a UPLC system coupled to a QTof mass spectrometer equipped with a C18 column (1.8 µm, 2.1 × 100 mm) maintained at 50 °C. The mobile phase consisted of water containing ammonium formate (A) and acetonitrile with formic acid (B), delivered at a flow rate of 0.2 mL min^{-1} with a total run time of 23 min. The dried extract (10 mg) was dissolved in methanol, and 5 µL was injected for analysis. Mass spectrometric detection was conducted using electrospray ionization in both positive and negative modes over an m/z range of 50–1200.[18]

Statistical Analysis
In MS-DIAL v3.82, raw LC-MS/MS data were first converted to ABF format using Abf converter 4.0.0 in conjunction with MS FileReader v2.2.62. Peak detection on the Orbitrap platform applied a minimum intensity threshold of 10,000 counts, a linear weighted moving average smoothing (level 4), and a preset minimum peak width. Detected features were aligned across samples with a 70 % spectral similarity cutoff, focusing on $[M+H]^+$ adducts. Compound annotation was performed against the RIKEN MS/MS human MSP library (http://prime.psc.riken.jp/compms/msdial/main.html#MSP, accessed on 5th July, 2025) in both positive and negative ionization modes. Pooled QC injections guided retention time correction and intensity normalization. Finally, only database matches within a ± 10 ppm mass error window were accepted for downstream qualitative profiling.

Results and Discussion

Fungal Endophytes from S. alata
A total of 7 fungal endophytes (SA-1 to SA-7) were successfully isolated from the leaf of *S. alata*. Morphological characterization was conducted based on colony color and surface texture observed on solid media. The findings are summarized in Table 1. Distinct colony pigmentation and surface texture variations were observed among the isolates, suggesting potential taxonomic diversity. Notably, isolates SA-3 and SA-6 exhibited pink pigmentation on the reverse side, while SA-2 showed the deepest coloration with a black underside. Surface morphology ranged from smooth to rough, with cotton-like textures predominating in several isolates.

Activities of endophytic fungi as antagonistic agents
The antagonistic potential of the seven endophytic fungal isolates isolated from the leaf of *S. alata* (SA-1 to SA-7) against *S. aureus*, *P. aeruginosa*, *C. albicans*, and *M. furfur* was evaluated by measuring zones of inhibition on plug agar assays i.e. agar disk diffusion method (immediately), and small fermentation assay i.e. agar well diffusion method (at three time points: day 14, day 18, and day 21), as in Table 2. At the plug-agar stage, only isolates SA-2 (6.46 mm against *S. aureus*), SA-6 (6.27 mm against *S. aureus*), and SA-7 (7.85 mm against *S. aureus*; 8.42 mm against *P. aeruginosa*) displayed antagonism. By day 14, the well diffusion method, *P. aeruginosa* became broadly susceptible: SA-1, SA-2, and SA-3 inhibited its growth with zones of 17.18 mm, 16.23 mm, and 16.14 mm, respectively. Notably, SA-3 also suppressed *M. furfur* (25.35 mm), and SA-5 inhibited both *P. aeruginosa* (15.24 mm) and *C. albicans* (19.85 mm). On day 18, *S. aureus* susceptibility peaked under SA-4 (16.55 mm) and SA-5 (13.93 mm), while *P. aeruginosa* was also strongly inhibited by SA-1 (17.50 mm), SA-3 (18.08 mm), SA-4 (17.95 mm), and SA-5 (18.12 mm). SA-7 exhibited delayed activity against *M. furfur* (20.53 mm). By day 21, only SA-3 and SA-5 maintained antagonism: SA-3 inhibited *P. aeruginosa* (14.79 mm) and *M. furfur* (14.97 mm), and SA-5 continued to suppress *P. aeruginosa* (17.21 mm) and *C. albicans* (21.20 mm). These results highlight isolate-specific and time-dependent antagonistic profiles, with SA-5 demonstrating the most sustained and broad-spectrum activity.

Molecular identification of SA-5
An endophytic fungal isolate, designated SA-5, was successfully isolated and subjected to molecular identification using ITS rRNA gene sequencing (Figure. 1). BLAST analysis of the ITS sequence against the NCBI GenBank database revealed a high degree of similarity between isolate SA-5 and members of the genus *Phomopsis* (Table 3). The isolate showed 100% query coverage, E-values of 0.0, and percentage identity ranging from 98.91% to 99.46%, indicating a reliable taxonomic match. The highest sequence similarity (99.46% identity) was observed with *Phomopsis* sp. isolate 76CG/L (GenBank accession no. GU066650.1), followed by several other *Phomopsis* isolates exhibiting similarly high identity values.

© 2026 the authors. This work is licensed under the Creative Commons Attribution 4.0 International License

ISSN 2616-0684 (Print)
ISSN 2616-0692 (Electronic)

Table 1: The surface morphology and color of fungal endophytes isolated from the leaf of *S. alata*

Code	Upper side	Bottom side	Morphology
SA-1		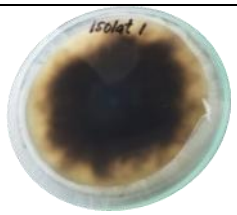	Colony Color - Top: Beige white - Bottom: brownish black Solid surface, rough like cotton.
SA-2			Colony Color - Top: Gray white to blackish - Bottom: deep black Solid surface, smooth.
SA-3	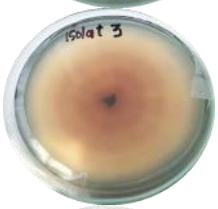		Colony Color - Top: tends to be White - Bottom: pink Solid surface, smooth like cotton
SA-4			Colony Color - Top: tends to be White - Bottom: white Thin, cotton-like surface
SA-5			Colony Color - Top: tends to be White - Bottom: beige to gray Thin, rough, textured surface.
SA-6			Colony Color - Top: tends to be White - Bottom: pink Thin, cotton-like surface
SA-7	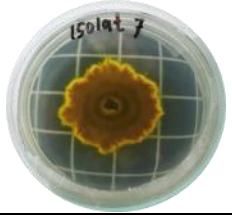	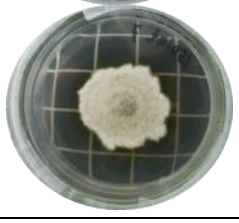	Colony Color - Top: beige white - Bottom: yellowish green Thick, rough, textured surface.

Additional closely related sequences included strains belonging to the genus *Diaporthe*, which showed slightly lower but still significant sequence identity values (98.91–98.92%). The occurrence of both *Phomopsis* and *Diaporthe* species among the closest matches reflects the well-documented close phylogenetic relationship between these genera. To further confirm the molecular identification, a phylogenetic tree was constructed based on ITS rDNA sequences using the neighbor-joining method (Figure. 2). The phylogenetic analysis revealed that isolate SA-5 clustered closely with reference strains of Phomopsis, forming a well-supported clade distinct from, yet closely related to, *Diaporthe* species. This clustering pattern corroborates the BLAST results and confirms the identification of isolate SA-5 as *Phomopsis* sp., an endophytic fungus associated with *S. alata*. A phylogenetic tree was reconstructed using the ITS region sequences from the endophytic isolate and 12 reference strains (Figure. 2). Two well-supported major clades emerged (bootstrap ≥ 90 %). The endophytic isolate (*Phomopsis* sp. 76C6/G1; GU066650.1) clustered with *P. maothokcampi* CGMCC 3.17588 (NR 147523.1) and *P. terminale* CGMCC 3.18183 (NR 147523.1).

This clade received 98 % bootstrap support, indicating a robust affiliation within the *Phomopsis* genus. Reference strains of *Diaporthe* formed a distinct sister clade, subdivided into two subgroups. Subgroup IIa comprised *D. phoenicicola* isolate FJ2-G-3 (MH504753.1) and *D. ychallo-2018* strain Y.H.Yeh 1103 (MK336527.1), with 95 % bootstrap

© 2026 the authors. This work is licensed under the Creative Commons Attribution 4.0 International License

ISSN 2616-0684 (Print)
ISSN 2616-0692 (Electronic)

Table 2: The diameter of the inhibition zone (mm) on the antagonism test from fungal endophytes isolated from the leaf of *S. alata*

	Diameter of inhibition zone (mm)			
	S. aureus	*P. aeruginosa*	*C. albicans*	*M. furfur*
Plug agar				
SA-1	ND	ND	ND	ND
SA-2	6.46	ND	ND	ND
SA-3	ND	ND	ND	ND
SA-4	ND	ND	ND	ND
SA-5	ND	ND	ND	ND
SA-6	6.27	ND	ND	ND
SA-7	7.85	8.42	ND	ND
Small fermentation assay on day 14				
SA-1	ND	17.18	ND	ND
SA-2	ND	16.23	ND	ND
SA-3	ND	16.14	ND	25.35
SA-4	ND	ND	ND	ND
SA-5	ND	15.24	19.85	ND
SA-6	ND	ND	ND	ND
SA-7	ND	ND	16.06	ND
Small fermentation assay on day 18				
SA-1	13.72	17.50	ND	ND
SA-2	ND	14.93	ND	ND
SA-3	ND	18.08	ND	ND
SA-4	16.55	17.95	ND	ND
SA-5	13.93	18.12	ND	ND
SA-6	ND	ND	ND	ND
SA-7	ND	ND	ND	20.53
Small fermentation assay on day 21				
SA-1	ND	ND	ND	ND
SA-2	ND	ND	ND	ND
SA-3	ND	14.79	ND	14.97
SA-4	ND	ND	ND	ND
SA-5	ND	17.21	21.2	ND
SA-6	ND	14.40	ND	ND
SA-7	ND	ND	ND	ND

Note: ND = not detected

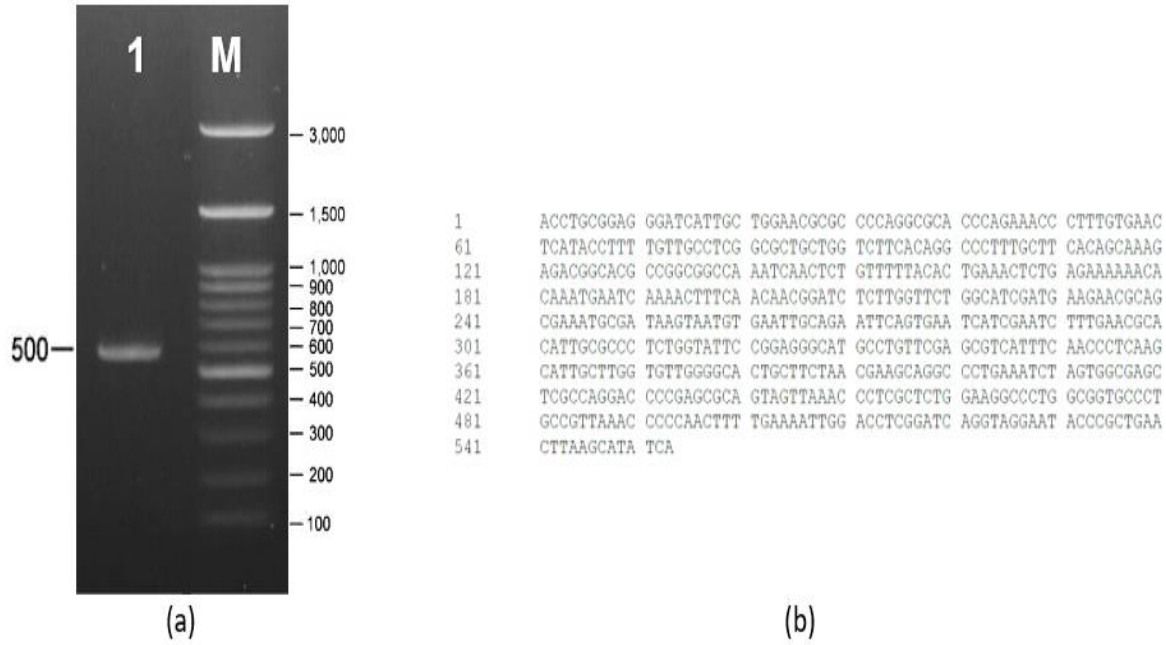

Figure 1: (a) Electrophoresis DNA of SA-5, (b) DNA sequence of ITS fragments of the fungal endophyte of SA-5 isolated from *S. alata*. Note: M= DNA Marker, 1= SA-5

© 2026 the authors. This work is licensed under the Creative Commons Attribution 4.0 International License

ISSN 2616-0684 (Print)
ISSN 2616-0692 (Electronic)

Table 3: ITS sequence similarity of fungal endophyte of SA-5 isolated from *S. alata*

Description	Scientific Name	Max Score	Query Cover	E value	Per. Identity	Acc. Len	Accession
Phomopsis sp. isolate 76CG/L was identified using rRNA gene sequencing, including the partial 18S rRNA gene, ITS1, complete 5.8S rRNA gene, ITS2, and partial 28S rRNA gene regions, which are commonly employed for reliable fungal identification and phylogenetic analysis.	*Phomopsis* sp. 76CG/L	1005	100%	0	99.46%	575	GU066650.1
Phomopsis sp. isolate 83DZ/L was identified based on rRNA gene sequencing, including the partial 18S rRNA gene, complete ITS1–5.8S–ITS2 region, and partial 28S rRNA gene, which together provide reliable molecular evidence for fungal identification and phylogenetic analysis.	*Phomopsis* sp. 83DZ/L	1000	100%	0	99.28%	576	GQ407101.1
Phomopsis sp. isolate 37GP/S was identified using rRNA gene sequencing, comprising the partial 18S rRNA gene, complete ITS1–5.8S–ITS2 region, and partial 28S rRNA gene, which collectively support accurate fungal identification and phylogenetic analysis.	*Phomopsis* sp. 37GP/S	998	100%	0	99.28%	568	GQ352477.1
Phomopsis sp. SAF-2022a isolate oblongitolus4_3 was molecularly identified based on rRNA gene sequencing, including partial ITS1, complete 5.8S rRNA and ITS2 regions, and a partial large subunit (28S) rRNA gene sequence, providing reliable support for fungal identification and phylogenetic placement.	*Phomopsis* sp. SAF-2022a	996	100%	0	99.27%	551	OP070553.1
Phomopsis sp. strain SN2 was identified using rRNA gene sequencing, comprising the partial small subunit (18S) rRNA gene, complete ITS1–5.8S–ITS2 region, and partial large subunit (28S) rRNA gene, supporting accurate fungal identification and phylogenetic analysis.	*Phomopsis* sp.	994	100%	0	99.10%	583	MT012101.1
Phomopsis sp. isolate NY6760b was identified based on rRNA gene sequencing, including the partial 18S rRNA gene, complete ITS1–5.8S–ITS2 region, and partial 28S rRNA gene, providing reliable molecular evidence for fungal identification and phylogenetic analysis.	*Phomopsis* sp. NY6760b	994	100%	0	99.10%	558	HM999921.1
Diaporthe sp. strain GMBCC2094 was molecularly identified using rRNA gene sequencing, comprising the partial small subunit (18S) rRNA gene, complete ITS1–5.8S–ITS2 region, and partial large subunit (28S) rRNA gene, supporting reliable taxonomic identification and phylogenetic analysis.	*Diaporthe* sp.	989	100%	0	98.92%	580	PX088274.1
Phomopsis sp. isolate 94NL/T was identified based on sequencing of the rRNA gene region, including the 18S rRNA gene, ITS1, 5.8S rRNA gene, ITS2, and 28S rRNA gene, providing reliable molecular support for fungal identification and phylogenetic analysis.	*Phomopsis* sp. 94NL/T	989	100%	0	98.92%	573	GU066662.1
Phomopsis sp. strain P47TD was molecularly identified using rRNA gene sequencing, comprising partial ITS1, complete 5.8S rRNA and ITS2 regions, and a partial large subunit (28S) rRNA gene, supporting accurate fungal identification and phylogenetic analysis.	*Phomopsis* sp.	989	100%	0	98.92%	556	MW543017.1
Diaporthe sp. strain GMBCC2098 was identified using rRNA gene sequencing, including the partial small subunit (18S) rRNA gene, complete ITS1–5.8S–ITS2 region, and partial large subunit (28S) rRNA gene, providing reliable molecular evidence for taxonomic identification and phylogenetic analysis.	*Diaporthe* sp.	989	100%	0	98.92%	594	PX088278.1
Diaporthe sp. isolate 49 C-2X (strain PPP-2020) was molecularly identified based on rRNA gene sequencing, including partial ITS1, complete 5.8S rRNA and ITS2 regions, and a partial large subunit (28S) rRNA gene, providing robust support for fungal identification and phylogenetic placement.	*Diaporthe* sp. 1 PPP-2020	987	100%	0	98.91%	554	MT556355.1

© 2026 the authors. This work is licensed under the Creative Commons Attribution 4.0 International License

ISSN 2616-0684 (Print)
ISSN 2616-0692 (Electronic)

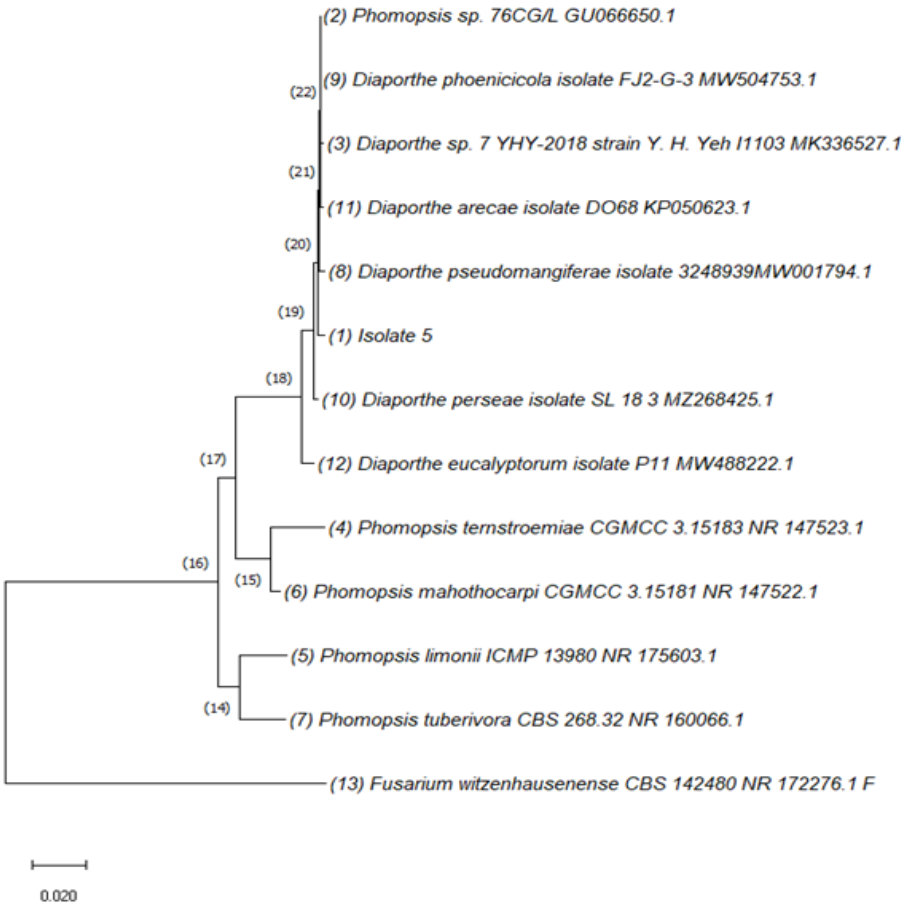

Figure 2: The phylogenetic tree of the ITS sequence of the fungal endophyte of SA-5 isolated from *S. alata* with its eleven closest strains, based on ITS DNA sequences, constructed using the neighbor-joining approach

support; and subgroup IIb contained multiple *D. eres* complex isolates (including SL 8 3 MZ264825.1, 3248939/MW001794.1) and *D. arecae* isolate DG68 (KP506823.1), supported by a 92 % bootstrap value. *Fusarium witzenhausenense* CBS 140680 (NR 172276.1) was used as the outgroup, anchoring the tree with a clear separation from *Phomopsis* and *Diaporthe* clades. The genetic-distance scale bar (0.020 substitutions per site) underscores the closer relatedness within each genus than the intergeneric divergence. These results confirm that the endophytic isolate belongs to the *Phomopsis* lineage and is most closely related to *P. maothokcampi* and *P. terminale.* At the same time, *Diaporthe* species form a separate, well-supported clade.

Bioactive screening of the fermentation broth of endophyte fungi of SA-5

The ethyl acetate extract of endophytic fungus SA-5 exhibited dose-dependent antibacterial and antifungal activity (Table 4, Figure. 3) Against *S. aureus*, the inhibition zone increased from 9.66±1.44 mm at 2.5 mg/mL to 14.37±1.20 mm at 20 mg/mL. A similar trend was observed for *P. aeruginosa*, rising from 8.32±1.00 mm to 15.18±1.02 mm over the same concentration range. No activity against *C. albicans* was detected at any concentration, whereas *M. furfur* was inhibited in a concentration-dependent manner (9.25±1.03 mm to 15.19±0.44 mm).

In contrast, the water extract showed no antibacterial activity at all tested doses. Antifungal activity against *C. albicans* appeared only at ≥10 mg/mL, with inhibition zones of 12.93±0.91 mm (10 mg/mL) and 15.33±1.66 mm (20 mg/mL). No inhibition of *M. furfur* was observed for the water extract. Gentamicin served as the positive control for bacteria, yielding zones of 19.75±0.69 mm (*S. aureus*) and 18.01±0.52 mm (*P. aeruginosa*) in the ethyl acetate series, and 18.49±0.45 mm and 17.73±0.33 mm in the water series. Ketoconazole inhibited *C. albicans* and *M. furfur* by 14.44±1.01 mm and 11.94±0.50 mm in the ethyl acetate series, and 14.12±0.81 mm and 11.36±0.27 mm in the water series.

Profile of active compounds from Phomopsis sp. (SA-5) Isolated from S. alata

Metabolite profiling of the endophytic fungus isolated from *S. alata* leaves yielded 29 detectable compounds. Table 5 presents the compounds extracted using ethyl acetate, while Table 6 summarizes those obtained with water as the extraction solvent. The chromatographic profile revealed distinct retention time variations ranging from 1.4 to 17.9 minutes in the samples analyzed (Figure. 4). The number of detected peaks, peak intensity, and peak area distinguished these variations in the ion chromatogram profiles at different retention times. Exploring the benefits of the fungus *Phomopsis* sp. has shown that this organism can produce secondary metabolites with broad applications in agriculture, medicine, and ecology. The compounds it generates can be employed to manufacture pharmaceuticals, chemical products, and other biological materials. Ecologically, the fungus plays a role in nutrient cycling within specific ecosystems. *Phomopsis* sp. is classified in the phylum *Ascomycota* and order *Diaporthales*, and is considered a synonym of the genus Diaporthe.[19] This fungus is characterized by colony formation, with the initial mycelium appearing white and then turning gray to light brown when grown on PDA, which aligns with the morphological results for SA-5.The fungus produces dense pycnidia that range from dark brown to black, globose to conical in shape, and are often distributed singly or in clusters.Some conidiophores are frequently branched and septate within the colony, and the conidia are hyaline (transparent).[20] Identifying endophytic fungal molecules underscores the importance of understanding plant microbial diversity and its potential benefits to human health. In this study, Forward ITS1 and Reverse ITS4 primers

© 2026 the authors. This work is licensed under the Creative Commons Attribution 4.0 International License

ISSN 2616-0684 (Print)
ISSN 2616-0692 (Electronic)

Table 4: Antimicrobial activity of the endophyte fungi of SA-5 isolated from *S. alata*. Data were shown in mean±SD.

	Diameter of inhibition zone (mm)			
Concentration (%)	*S. aureus*	*P. aeruginosa*	*C. albicans*	*M. furfur*
Ethyl acetate extract				
2.5	9.66±1.44	8.32±1.00	ND	9.25±1.03
5.0	12.00±0.31	10.84±0.74	ND	11.24±0.99
10	13.28±0.45	10.97±1.34	ND	12.67±3.15
20	14.37±1.20	15.18±1.02	ND	15.19±0.44
Gentamicin	19.75±0.69	18.01±0.52	ND	-
Ketoconazole	-	-	14.44±1.01	11.94±0.50
Water extract				
2.5	ND	ND	ND	ND
5.0	ND	ND	ND	ND
10	ND	ND	12.93±0.91	ND
20	ND	ND	15.33±1.66	ND
Gentamicin	18.49±0.45	17.73±0.33	-	-
Ketoconazole	-	-	14.12±0.81	11.36±0.27

Note: Gentamicin (10 µg/disc), ketoconazole (30 µg/disc), and ND = not detected

Table 5: Profile of active compounds in the ethyl acetate extract of *Phomopsis* sp.

Retention Time	Molecular Weight (g/mol)	Molecule Formula	Metabolite name	Ontology	Biological activities
1.386	273.12134	$C_{15}H_{12}O_5$	Naringenin	Flavanones	Anticancer,[43] anti-inflammatory,[44] antibacterial[28] and antiviral.[45]
1.407	118.08747	$C_5H_{11}NO_2$	Betaine	Alpha amino acids	Anti-inflammatory.[46]
1.436	204.08501	$C_9H_{17}NS_2$	7-Methylsulfenylheptyl isothiocyanate	Isothiocyanates	No activities
1.447	274.1904	$C_{17}H_{23}NO_2$	4-hydroxy-2-octylquinoline 1-oxide	4-hydroxy-2-alkyl quinolines	No activities
1.468	150.07928	$C_6H_7N_5$	3-Methyladenine	6-aminopurines	No activities
1.489	149.10825	$C_9H_{12}N_2$	Nornicotine	Pyrrolidinylpyridines	Neuroprotective.[47]
1.696	124.04147	$C_6H_5NO_2$	Nicotinic acid	Pyridinecarboxylic acids	Neuroprotective.[48,49]
1.851	147.0455	$C_9H_6O_2$	Coumarin	Coumarins and derivatives	Antioxidant, anticancer, anti-inflammatory, and antimicrobial.[29]
1.851	165.05608	$C_9H_8O_3$	p-Coumaric acid	Hydroxycinnamic acids	Antimicrobial.[30]
1.872	191.08601	$C_{10}H_{10}N_2O_2$	Chrysogine	Quinazolines	Antimicrobial, anticancer,[31] and antibacterial.[32,33,50]
2.223	195.08066	$C_{14}H_{10}O$	Anthrone	Anthracenes	Antimicrobial.[34]
5.847	247.10907	$C_{13}H_{14}N_2O_3$	N-Acetyltryptophan	N-acyl-alpha amino acids	Inhibit AChE/Anti cholinesterase.[51]
8.034	1075.5708	$C_{53}H_{86}O_{22}$	Ardisiacrispin B	Triterpenoids	Anti-inflammatory.[52]

© 2026 the authors. This work is licensed under the Creative Commons Attribution 4.0 International License

ISSN 2616-0684 (Print)
ISSN 2616-0692 (Electronic)

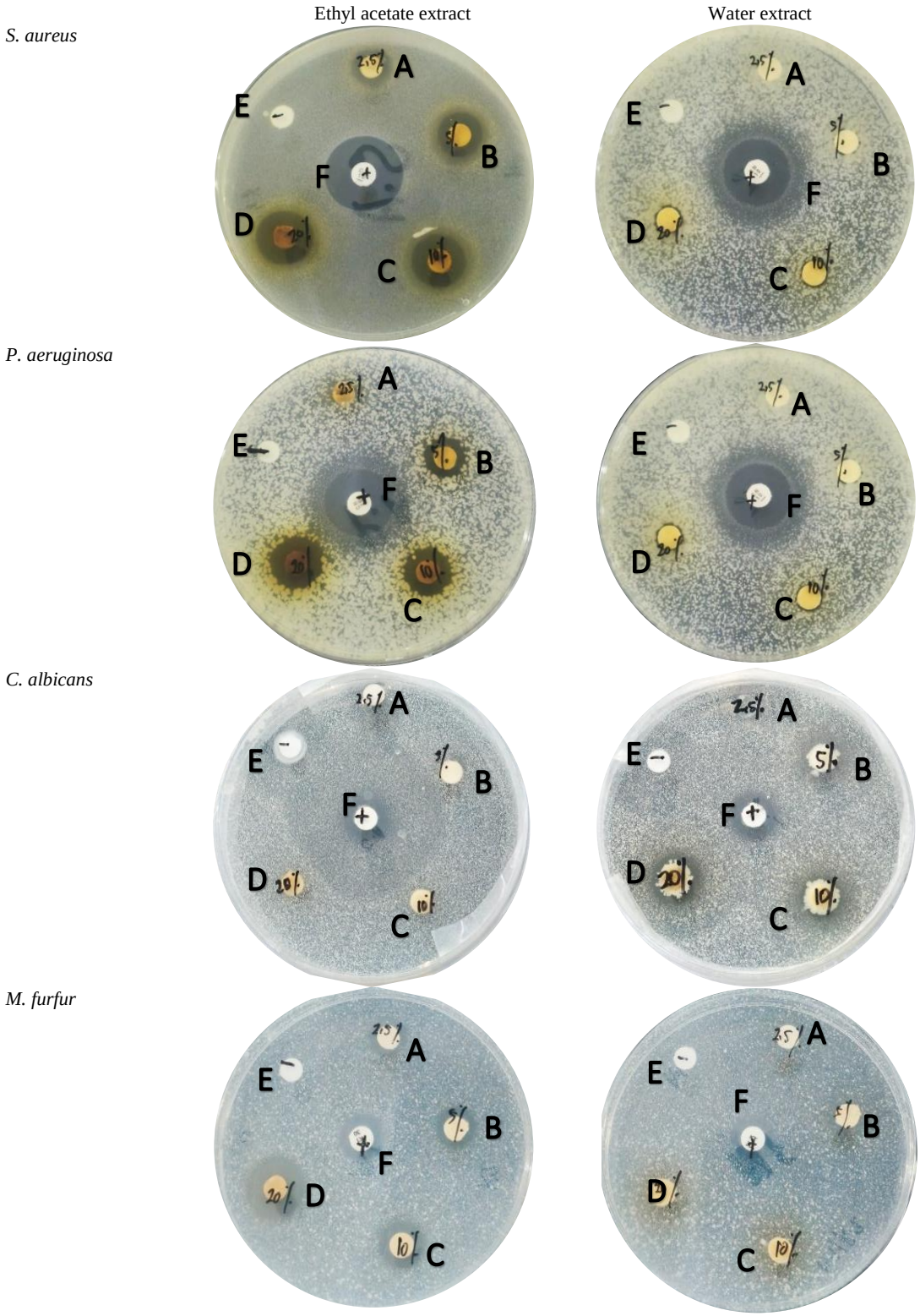

Figure 3: The comparison inhibition zone between ethyl acetate and the water extract of the endophyte fungi of SA-5 isolated from *S. alata* against two bacteria and two fungi.

© 2026 the authors. This work is licensed under the Creative Commons Attribution 4.0 International License

ISSN 2616-0684 (Print)
ISSN 2616-0692 (Electronic)

Table 6: Profile of active compounds in the water extract of *Phomopsis* sp.

Retention Time	Molecular Weight (g/mol)	Molecule Formula	Metabolite name	Ontology	Biological activities
1.457	272.17853	$C_{16}H_{21}N_3O$	2-[(2-metilaminoetil)(p-metoksibenzil)amino] piridina	2-benzylaminopyridines	No activities
1.478	254.16644	$C_{16}H_{19}N_3$	Anabasamine	Bipyridines and oligopyridines	Insecticide.[53]
1.83	150.07744	$C_6H_7N_5$	3-methyladenine	Purines and purine derivatives	Inhibitor autophagy.[54]
1.83	216.09088	$C_{10}H_9N_5O$	Kinetin	6-alkylaminopurines	Antiaging.[55]
1.861	123.04336	$C_7H_6O_2$	4-hydroxybenzaldehyde	Hydroxybenzaldehydes	Antiparasitic[56] and antioxidant.[57]
2.006	185.0946	$C_7H_{12}N_4O_2$	Diketometribuzin	Pyrimidones	Herbicide.[58]
4.012	295.17612	$C_{19}H_{22}N_2O$	Cinchonine	Cinchona alkaloids	Anticancer[59] and antimalaria.[59]
4.167	247.12921	$C^{15}H_{18}O_3$	Desmotroposantonin	Naphthofurans	Anticancer.[60]
4.209	146.06007	C_9H_7NO	Indole-3-carboxaldehyde	Indoles	Antimicrobial.[35]
4.364	190.05362	$C_{10}H_7NO_3$	Kynurenic acid	Quinoline carboxylic acids	Neuroprotective and anticonvulsant.[61]
4.519	265.15549	$C_{14}H_{20}N_2O_3$	Asam (2S)-2-[(2-amino-3-metilbutanoil) amino]-3-fenilpropanoat	Dipeptides	No activities
4.653	377.13657	$C_{17}H_{20}N_4O_6$	Lyxoflavin	Flavins	No activities
4.761	265.15765	$C_{14}H_{20}N_2O_3$	Feruloylputrescine	Hydroxycinnamic acids and derivatives	Bactericide.[36]
5.408	286.20563	$C_{17}H_{19}NO_3$	Piperine	Alkaloids and derivatives	Anti-inflammation, anticancer, and bioenhancer.[62]
6.421	489.35965	$C_{30}H_{48}O_5$	Asiatic acid	Triterpenoids	Wound healing,[63] antimicrobial,[37] anticancer,[64] neuroprotection and inflammation.[65]
12.154	387.31186	$C_{22}H_{42}O_5$	Bourgeanic acid	3-(3-hydroxyalkanoyloxy) alkanoic acids	No activities

were used to amplify fungal DNA isolated from the leaves of *S. alata* (Figure. 1). Agarose gel electrophoresis analysis revealed DNA fragments of the expected size for ITS amplification. Comparative study of these sequences against known ITS databases indicated similarity with the genus *Phomopsis*. Evolutionary relationships were then inferred using the two-parameter Kimura method.[21] This analysis involved eleven strains from the NCBI database. Sites with data coverage below 95% were removed. For alignment gaps under 5%, missing data and ambiguous bases were permitted at any position (optional partial deletion). Phylogenetic trees were constructed using MEGA version 11.[22] The increasing number of bacterial species resistant to drugs and disinfectants has led to higher morbidity and mortality rates. In the year 2025, WHO released its first report on shortages of drugs and diagnostics for invasive fungal infections. The WHO noted that infections such as oral and vaginal thrush (*Candida* spp.) are becoming increasingly unresponsive to treatment. Diagnostic tools and therapies are minimal, especially in low- and middle-income countries. The WHO considers this a serious threat to immunocompromised patients and has called for immediate, innovative, research and development efforts.[23] In response, researchers are searching for natural metabolites with antimicrobial properties.

This study evaluated the antimicrobial activity of *Phomopsis* sp. fungal extracts against the pathogens *P. aeruginosa*, *S. aureus*, *C. albicans*, and *M. furfur*. Both the aqueous and ethyl acetate extracts of *Phomopsis sp*. produced inhibition zones against all four test organisms. However, the ethyl acetate extract showed no activity against *C. albicans*, whereas the aqueous extract inhibited only *C. albicans*. Usually Gram-positive bacteria are quite sensitive to antibacterial activity. This resistance of Gram-negative bacteria can be caused by the permeability of the cell wall to bacterial agents, genetically able to overcome various mechanisms of resistance, mutations in chromosomal genes regulating the expression of resistance genes and the acquisition of foreign resistance genes through plasmids, transposons and bacteriophages.[24] Meanwhile, the strong antifungal activity of endophytic fungi is caused by the presence of alkaloids such as cytochalasin, terpenoids, polyketides, propanoic acid, piliformic acid, cordycepin A, ferulic acid, etc. in their exudates.[25] These results indicate that the choice of solvent for extracting *Phomopsis sp*. metabolites significantly affects antimicrobial efficacy The observed inhibition zones against bacterial and fungal pathogens suggest that *Phomopsis* sp. extracts hold promise as antimicrobial agents. Our findings support earlier reports of antimicrobial activity in *Phomopsis* sp. extracts isolated from various host plants.[26,27]The antimicrobial spectrum of the ethyl acetate extract of *Phomopsis* sp. is broader than that of the aqueous extract. This indicates that the ethyl acetate fraction contains a higher concentration of bioactive metabolites, as demonstrated by LC–MS/MS analysis. Several compounds identified in the ethyl acetate extract, including naringenin, coumarin, chrysogine, p-coumaric acid, and anthrone, have been associated with antimicrobial activity.

The research conducted by [28] revealed that naringenin possesses significant antibacterial efficacy against *E. faecalis*, a Gram-positive bacterium frequently inhabiting the gastrointestinal system of people and animals, and capable of inducing severe illnesses. Homology modeling and molecular docking analyses demonstrated that naringenin interacts with the active site of β-ketoacyl-acyl carrier protein synthase III, a crucial enzyme that initiates bacterial fatty acid production. The combination of naringenin with oxacillin or cloxacillin exhibited synergistic antibacterial activity against MRSA.[28]

© 2026 the authors. This work is licensed under the Creative Commons Attribution 4.0 International License

ISSN 2616-0684 (Print)
ISSN 2616-0692 (Electronic)

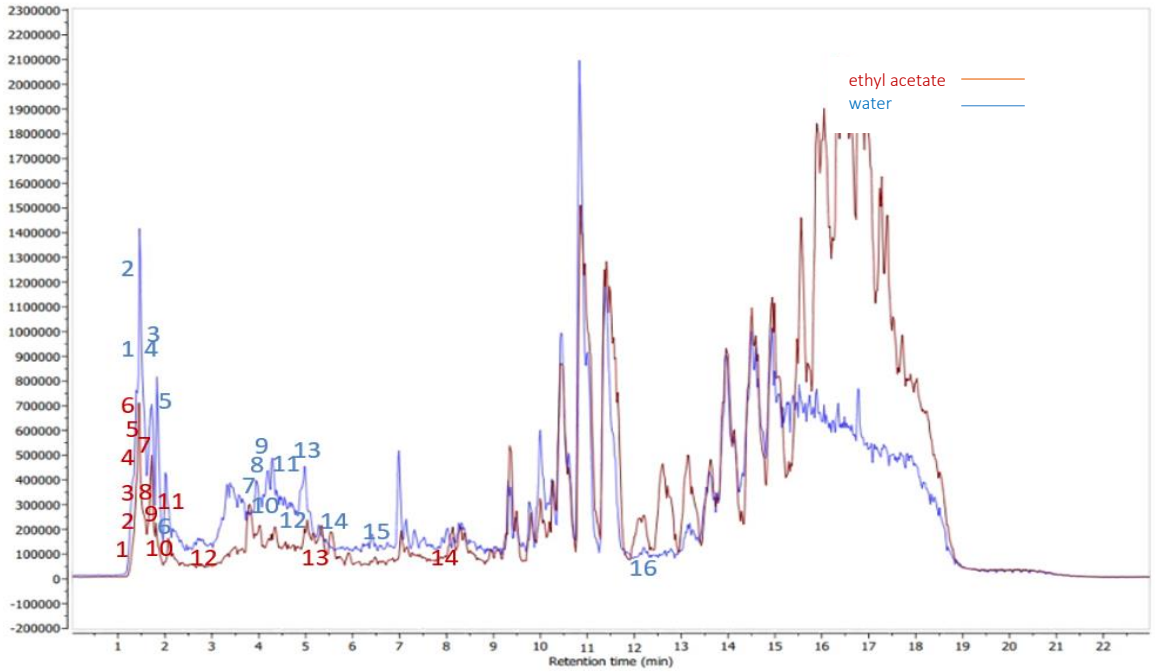

Figure 4: LC-MS/MS chromatograms of the ethyl acetate (red line) and water (blue line) extracts obtained from endophytic fungi SA-5, *Phomopsis* sp.

In the study [29] coumarin was effective against several pathogenic bacteria, including *E. faecium, S. aureus, K. pneumoniae, Acinetobacter baumannii*, *P. aeruginosa*, and *E. species*. In addition, coumarin exhibited antifungal activity against *C. albicans* and four other pathogenic fungi, namely *F. oxysporum, A. flavus*, *Aspergillus niger*, and *Cryptococcus neoformans*.[29] The study de Sousa 3^0 reported the activity of p-coumaric acid against *Bacillus cereus* and *B. subtilis*, as well as *E. coli*, *Salmonella* spp., *Listeria* spp., and *Clostridium* spp.[30] Similarly, investigations [31-33]demonstrated that chrysogine is effective against bacterial pathogens such as *S. aureus*, *Bacillus* spp., *K. pneumoniae*, and *P. aeruginosa*, as well as the fungal pathogen *C. albicans*.[31-33] In addition, anthrone has been shown to possess antimicrobial activity against *E. coli*, *Salmonella* spp., *Vibrio cholerae*, *S. aureus*, *S. typhimurium*, and *C. albicans.*[34] Several compounds with antimicrobial potential were also identified in the aqueous extract, including indole-3-carboxaldehyde, feruloylputrescine, and asiatic acid. According to [35] indole-3-carboxaldehyde is active against *S. aureus*, MRSA, *E. coli*, *Bacillus subtilis*, and *C. albicans*.[35] Feruloylputrescine was reported to inhibit aflatoxin B1 production in *Aspergillus* spp.[36] Moreover, asiatic acid demonstrated antimicrobial properties against *Clostridium difficile*, *S. aureus*, *E. faecalis*, and *P. aeruginosa* in its biofilm form.[37] These metabolites likely act directly or indirectly to influence the observed inhibition zones. The bioactivity of fungal secondary metabolites has been associated with their ability to interfere with multiple microbial processes, including cell-wall synthesis, ergosterol biosynthesis, membrane depolarization, protein synthesis, nucleic acid synthesis, and other key metabolic pathways.[38,39]

Recently, numerous fungal secondary metabolites have been developed into novel therapeutic agents, most notably antibiotics. Although a wide range of compounds from *Diaporthe* and *Phomopsis* species have been reported regarding isolation, structure elucidation, and *in vitro* activity, in-depth investigations into their pharmacological mechanisms and drug development potential remain limited.[40] Our metabolite profiling is consistent with findings by [41,42] which identified alkaloids, terpenoids, pyrones, and polyketides as the principal classes of bioactive compounds produced by *Phomopsis*. These chemical groups exhibit diverse biological activities, including anti-inflammatory, antibacterial, and anticancer effects, thus highlighting their potential for future pharmaceutical applications.[41,42]

Diaporthe (*Phomopsis*) fungi represent an important resource for natural product discovery and biosynthetic research. Research on *Diaporthe* (*Phomopsis*) has been primarily focused on the isolation and structural characterization of new natural compounds, accompanied by preliminary bioactivity screening. However, investigations into their biosynthetic genes and enzymes remain scarce, and the bioactivity of most reported metabolites has only been evaluated under *in vitro* conditions.

Conclusion

In this study, the endophytic fungus strain SA-5 exhibited 99.46% DNA sequence similarity to *Phomopsis* sp. LC–MS/MS analysis of its ethyl acetate and aqueous extracts identified 29 metabolites, including antroquinone, asiatic acid, coumarin, crisotin, feruloylputrescine, indole-3-carboxaldehyde, and naringenin. Several of these compounds demonstrated antimicrobial activity, notably by inhibiting the growth of *S. aureus*, *P. aeruginosa*, *C. albicans*, and *M. furfur*. These findings suggest that the SA-5 strain of *Phomopsis* sp. represents a promising candidate for further investigation as a potential source of novel antimicrobial agents. To fully realize the therapeutic potential of these fungi, further studies are warranted to elucidate the biosynthetic pathways and pharmacological mechanisms of their highly active metabolites.

Conflict of Interest

The authors declare no conflict of interest.

Authors' Declaration

The authors hereby declare that the work presented in this article is original and that any liability for claims relating to the content of this article will be borne by them.

Acknowledgements

The authors gratefully acknowledge the Ministry of Health of the Republic of Indonesia for funding this research under Tugas Belajar Sumber Daya Manusia Kesehatan Tingkat Pusat 2024 scheme (HK.01.07/F.I/5962/2024).

© 2026 the authors. This work is licensed under the Creative Commons Attribution 4.0 International License

References

1. Burhamzah R, Alam G, Rante H. Characterization of antibacterial-producing endophytic fungi of *Syzygium polyanthum* leaves. Infect Disord Drug Targets. 2020;20(4):448-454.
2. Fadiji AE, Babalola OO. Elucidating mechanisms of endophytes used in plant protection and other bioactivities with multifunctional prospects. Front Bioeng Biotechnol. 2020;8:e467.
3. Gurgel RS, de Melo Pereira DÍ, Garcia AVF, Fernandes de Souza AT, Mendes da Silva T, de Andrade CP, Lima da Silva W, Nunez CV, Fantin C, de Lima Procópio RE, Albuquerque PM. Antimicrobial and antioxidant activities of endophytic fungi associated with *Arrabidaea chica* (Bignoniaceae). J Fungi. 2023;9(8):e864.
4. Shurigin V, Alaylar B, Davranov K, Wirth S, Bellingrath-Kimura SD, Egamberdieva D. Diversity and biological activity of culturable endophytic bacteria associated with marigold (*Calendula officinalis* L.). AIMS Microbiol. 2021;7(3):336-353.
5. Trivedi P, Leach JE, Tringe SG, Sa T, Singh BK. Plant–microbiome interactions: From community assembly to plant health. Nat Rev Microbiol. 2020;18(11):607-621.
6. Omomowo IO, Amao JA, Abubakar A, Ogundola AF, Ezediuno LO, Bamigboye CO. A review on the trends of endophytic fungi bioactivities. Sci Afr. 2023;20:e01594.
7. Gupta A, Meshram V, Gupta M, Goyal S, Qureshi KA, Jaremko M, Shukla KK. Fungal endophytes: Microfactories of novel bioactive compounds with therapeutic interventions; A comprehensive review on the biotechnological developments in the field of fungal endophytic biology over the last decade. Biomol. 2023;13(7):e1038.
8. El-Bondkly EAM, El-Bondkly AAM, El-Bondkly AAM. Marine endophytic fungal metabolites: A whole new world of pharmaceutical therapy exploration. Heliyon. 2021;7(3).
9. Amaliah R, Basarang M, Nurhidayat N. Literature review of the antifungal potential of *Cassia alata* L. leaves against pathogenic fungi in humans. Jurnal Medika. 2020;5:1-8.
10. Sharma P, Pandey D, Rizvi A, Gupta A. Antimicrobial activity of *Cassia alata* from Raipur region against clinical and MTCC isolates. Int J Curr Microbiol App Sci. 2015;4(1):330-339.
11. Fitriani IR, Fitriana F, Nuryanti S. Antibacterial activity of ethanol extract of ketepeng cina leaves (*Cassia alata* L.) Against some bacteria that cause skin infections. Makassar Nat. Prod. J. 2023;1(4):22-28.
12. Gama AMP, Subakir S, Suhardjono S. *In vitro* comparison of candle bush (*cassia alata*, linn.) Leaves extract with ketoconazole 2% to inhibit the growth of *Malassezia furfur* in *Pityriasis versicolor*: Faculty of Medicine; 2011.
13. Muhammad SL, Wada Y, Mohammed M, Ibrahim S, Musa KY, Olonitola OS, Ahmad MH, Mustapha S, Abdul Rahman Z, Sha'aban A. Bioassay-guided identification of bioactive compounds from *Senna alata* L. against Methicillin-Resistant *Staphylococcus aureus*. Appl Microbiol. 2021;1(3):520-536.
14. Kusmiati K, Fanani A, Nurkanto A, Purnaningsih I, Mamangkey J, Ramadhani I, Nurcahyanto DA, Simanjuntak P, Afiati F, Irawan H, Puteri AL, Ewaldo MF, Juanssilfero AB. Profile and in silico analysis of metabolite compounds of the endophytic fungus *Alternaria alternata* K-10 from *Drymoglossum piloselloides* as antioxidants and antibacterials. Heliyon. 2024;10(6):e27978.
15. Haq N, Sjahril R, Rante H, Massi MN, Yustisia I, Pattellongi I. Molecular characterization of endophytic fungi from the leaves of beruwas laut (*Scaevola taccada* (gaertn.) Roxb.) as antibacterial producer. Trop J Nat Prod Res. 2024;8(1):5845-5851.
16. Rütten A, Kirchner T, Musiol-Kroll EM. Overview on strategies and assays for antibiotic discovery. Pharmaceuticals. 2022;15(10):e1302.
17. Eltawaty SI, Suliman MB, El-Hddad S. Chemical composition, and antibacterial and antifungal activities of crude extracts from *Pistacia lentiscus* L. fruit. Trop J Nat Prod Res. 2023;7(9):4049-4054.
18. Burhan A, Ratnadewi D, Setiyono A, Astuti RI, Umar AH. Phytochemical profiling of *Hippobroma longiflora* leaf extract using LC-MS/MS analysis and pharmacological potential. Egypt J Chem. 2024;67(7):83-90.
19. Norphanphoun C, Gentekaki E, Hongsanan S, Jayawardena R, Senanayake I, Manawasinghe I, Abeywickrama P, Bhunjun C, Hyde K. Diaporthe: Formalizing the species-group concept. Mycosphere. 2022;13(1):752-819.
20. Zhu Y-Q, Ma C-Y, Xue H, Piao C-G, Li Y, Jiang N. Two new species of *Diaporthe* (Diaporthaceae, Diaporthales) in China. MycoKeys. 2023;95:209-228.
21. Kimura M. A simple method for estimating evolutionary rates of base substitutions through comparative studies of nucleotide sequences. J Mol Evol. 1980;16(2):111-120.
22. Tamura K, Stecher G, Kumar S. MEGA11: Molecular evolutionary genetics analysis version 11. Mol Biol Evol. 2021;38(7):3022-3027.
23. WHO. WHO issues its first-ever reports on tests and treatments for fungal infections. World Health Organization; 2025.
24. Nazir A, Nazir A, Zuhair V, Aman S, Sadiq SUR, Hasan AH, Tariq M, Rehman LU, Mustapha MJ, Bulimbe DB. The Global Challenge of Antimicrobial Resistance: Mechanisms, Case Studies, and Mitigation Approaches. Health Sci. Rep. 2025;8(7):e71077.
25. Xu K, Li X-Q, Zhao D-L, Zhang P. Antifungal Secondary Metabolites Produced by the Fungal Endophytes: Chemical Diversity and Potential Use in the Development of Biopesticides. Front. Microbiol. 2021; 12: 2021.
26. Chen Y, Wang H, Ke X, Sang Z, Kuang M, Peng W, Tan J, Zheng Y, Zou Z, Tan H. Five new secondary metabolites from an endophytic fungus *Phomopsis* sp. SZSJ-7B. Front Plant Sci. 2022;13:e1049015.
27. Latifah T. Screening of antimicrobial activity of endophytic fungi *Phomopsis* sp. *Strains pcl-o-35* and *neopestalotiopsis* sp. *Pcl-o-36* strain isolated from peronema canescens jack: Universitas Islam Indonesia; 2024.
28. Jadimurthy R, Jagadish S, Nayak SC, Kumar S, Mohan CD, Rangappa KS. Phytochemicals as invaluable sources of potent antimicrobial agents to combat antibiotic resistance. Life. 2023;13(4):e948.
29. Annunziata F, Pinna C, Dallavalle S, Tamborini L, Pinto A. An overview of coumarin as a versatile and readily accessible scaffold with broad-ranging biological activities. J Mol Sci. 2020;21(13):e4618.
30. de Sousa Silveira Z, Macêdo NS, Menezes Dantas Dd, Rodrigues dos Santos Barbosa C, Muniz DF, Morais Oliveira-Tintino CDd, Relison Tintino S, Alencar GG, Marinho ES, Rocha MNd, Marinho MM, Santos HSd, Coutinho HDM, Cunha FABd, Silva MVd. Evaluation of the antibacterial and inhibitory activity of the NorA and TetK efflux pumps of *Staphylococcus aureus* by p-coumaric acid. Microb Pathog. 2025;200:e107318.
31. Deng Z, Li J, Zhu P, Wang J, Kong Y, Hu Y, Cai J, Dong C. Quinazolinones as potential anticancer agents: Synthesis and action mechanisms. Biomol. 2025;15(2):e210.
32. Li Z, Zhao L, Bian Y, Li Y, Qu J, Song F. The antibacterial activity of quinazoline and quinazolinone hybrids. Curr Top Med Chem. 2022;22(12):1035-1044.
33. Osarumwense O, Edema M, Usifoh C. Synthesis and antibacterial activities of quinazolin-4(3h)-one, 2-methyl-4(3h)-quinazolinone and 2–phenyl-4(3h)-quinazolinone. Int J Bio Pharm Sci Arc. 2021;1:077-084.
34. Asamenew G, Bisrat D, Mazumder A, Asres K. *In vitro* antimicrobial and antioxidant activities of anthrone and chromone from the latex of *Aloe harlana* Reynolds. Phytother Res. 2011;25(12):1756-1760.
35. Shirinzadeh H, Altanlar N, Yucel N, Ozden S, Suzen S. Antimicrobial evaluation of indole-containing hydrazone derivatives. Z Naturforsch C J Biosci. 2011;66(7-8):340-344.

© 2026 the authors. This work is licensed under the Creative Commons Attribution 4.0 International License

36. Aksenov AA, Blacutt A, Ginnan N, Rolshausen PE, A VM, Lotfi A, E CG, Ramasamy M, Zuniga C, Zengler K, Mandadi KK, McCollum G, Dorrestein PC, Roper MC. Spatial chemistry of citrus reveals molecules bactericidal to *Candidatus Liberibacter* asiaticus. Sci Rep. 2024;14(1):e20306.
37. Idris FN, Mohd Nadzir M. Comparative studies on different extraction methods of *Centella asiatica* and extracts bioactive compounds effects on antimicrobial activities. Antibiotics (Basel). 2021;10(4):e457.
38. Osset-Trénor P, Pascual-Ahuir A, Proft M. Fungal drug response and antimicrobial resistance. J Fungi. 2023;9(5):e565.
39. Zhang F, Cheng W. The mechanism of bacterial resistance and potential bacteriostatic strategies. Antibiotics. 2022;11(9):e1215.
40. Xu T-C, Lu Y-H, Wang J-F, Song Z-Q, Hou Y-G, Liu S-S, Liu C-S, Wu S-H. Bioactive secondary metabolites of the genus *Diaporth*e and anamorph *Phomopsis* from terrestrial and marine habitats and endophytes: 2010–2019. Microorganisms. 2021;9(2):e217.
41. Jiang L, Ma Q, Li A, Sun R, Tang G, Huang X, Pu H. Bioactive secondary metabolites produced by fungi of the genus *Diaporthe* (*Phomopsis*): Structures, biological activities, and biosynthesis. Arab J Chem. 2023;16(9):e105062.
42. Wei W, Khan B, Dai Q, Lin J, Kang L, Rajput NA, Yan W, Liu G. Potential of secondary metabolites of *Diaporthe* species associated with terrestrial and marine origins. J Fungi. 2023;9(4):e453.
43. Liu W, Zheng W, Cheng L, Li M, Huang J, Bao S, Xu Q, Ma Z. Citrus fruits are rich in flavonoids for immunoregulation and potential targeting ACE2. Nat Prod Bioprospect. 2022;12(1):4.
44. Stabrauskiene J, Kopustinskiene DM, Lazauskas R, Bernatoniene J. Naringin and naringenin: Their mechanisms of action and the potential anticancer activities. Biomedicines. 2022;10(7):e1686.
45. Cai J, Wen H, Zhou H, Zhang D, Lan D, Liu S, Li C, Dai X, Song T, Wang X, He Y, He Z, Tan J, Zhang J. Naringenin: A flavanone with anti-inflammatory and anti-infective properties. Biomed Pharmacother. 2023;164:e114990.
46. Zhao G, He F, Wu C, Li P, Li N, Deng J, Zhu G, Ren W, Peng Y. Betaine in inflammation: Mechanistic aspects and applications. Front Immunol. 2018;9:e1070.
47. Ahmed EM, Khalil NA, Ramadan E, Tharwat T, Ali MA, Mahmoud Z. Synthesis and biological evaluation of new nicotinic acid derivatives as potential anti-inflammatory agents with enhanced gastric safety profile. Bioorg Chem. 2024;144:e107136.
48. Samad N, Manzoor N, Batool A, Noor A, Khaliq S, Aurangzeb S, Bhatti SA, Imran I. Protective effects of niacin following high fat rich diet: An *in-vivo* and *in-silico* study. Sci Rep. 2023;13(1):e21343.
49. Samad N, Hameed A, Manzoor N, Shoukat S, Irfan A, Shazly GA, Khalid A, Ejaz U, Khaliq S, Mateev E, Bin Jardan YA. Antioxidant and neuro-modulatory effects of niacin prevent D-galactose-induced behavioral deficits and memory impairment. Exp Gerontol. 2024;198:e112624.
50. Asif M. Chemical characteristics, synthetic methods, and biological potential of quinazoline and quinazolinone derivatives. Int J Med Chem. 2014;2014(1):e395637.
51. Orhan IE, Kucukboyaci N, Calis I, Cerón-Carrasco JP, den-Haan H, Peña-García J, Pérez-Sánchez H. Acetylcholinesterase inhibitory assessment of isolated constituents from *Salsola grandis* Freitag, Vural & Adıgüzel and molecular modeling studies on *N*-acetyltryptophan. Phytochem Lett. 2017;20:373-378.
52. Zhou W, Yang G, Wen Y, Xiao Q, Sun L, Li Y, Gong Z, Wang Y. Metabolites-based network pharmacology to preliminarily verify *in vitro* anti-inflammatory effect of ardisiacrispin B. Int J Mol Sci. 2023;24(23):e17059.
53. Fowsiya J, Madhumitha G. A review of bioinsecticidal activity and mode of action of plant derived alkaloids. Research J Pharm Tech. 2020;13(2):963-973.
54. Pasquier B. Autophagy inhibitors. Cell Mol Life Sci. 2016;73(5):985-1001.
55. Le Bris M. Hormones in growth and development. Reference Module in Life Sciences: Elsevier; 2017.
56. Lee J, Choi JW, Han HY, Kim WS, Song HY, Byun EB, Byun EH, Lee YH, Yuk JM. 4-hydroxybenzaldehyde restricts the intracellular growth of toxoplasma gondii by inducing SIRT1-mediated autophagy in macrophages. Korean J Parasitol. 2020;58(1):7-14.
57. Ha JH, Lee DU, Lee JT, Kim JS, Yong CS, Kim JA, Ha JS, Huh K. 4-Hydroxybenzaldehyde from *Gastrodia elata* B1. is active in the antioxidation and GABAergic neuromodulation of the rat brain. J Ethnopharmacol. 2000;73(1-2):329-333.
58. Albero B, Fernández MD, García-Gómez C, Pérez RA. Rapid determination of metribuzin and three major transformation products in soil and plant by Gas Chromatography–Tandem Mass Spectrometry. Separations. 2022;9(12):e386.
59. Parveen S, Maurya N, Meena A, Luqman S. Cinchonine: A versatile pharmacological agent derived from natural cinchona alkaloids. Curr Top Med Chem. 2024;24(4):343-363.
60. Khazir J, Singh PP, Reddy DM, Hyder I, Shafi S, Sawant SD, Chashoo G, Mahajan A, Alam MS, Saxena AK, Arvinda S, Gupta BD, Kumar HMS. Synthesis and anticancer activity of novel spiro-isoxazoline and spiro-isoxazolidine derivatives of α-santonin. Eur J Med Chem. 2013;63:279-289.
61. Walczak K, Wnorowski A, Turski WA, Plech T. Kynurenic acid and cancer: Facts and controversies. Cell Mol Life Sci. 2020;77(8):1531-1550.
62. Singh A, Singh DK, Kharwar RN, White JF, Gond SK. Fungal endophytes as efficient sources of plant-derived bioactive compounds and their prospective applications in natural product drug discovery: Insights, avenues, and challenges. Microbe. 2021;9(1):e197.
63. Diniz LRL, Calado LL, Duarte ABS, de Sousa DP. *Centella asiatica* and its metabolite asiatic acid: Wound healing effects and therapeutic potential. Metabolites. 2023;13(2):e 276.
64. Chen R, Zhang W, Zhang M, Liu W, Feng W, Zhang Y. Asiatic acid in anticancer effects: Emerging roles and mechanisms. Front Pharmacol. 2025;16:e 1545654.
65. Lv J, Sharma A, Zhang T, Wu Y, Ding X. Pharmacological review on asiatic acid and its derivatives: A potential compound. SLAS Technol. 2018;23(2):111-127.

© 2026 the authors. This work is licensed under the Creative Commons Attribution 4.0 International License